AIAA JOURNAL
Vol. 34, No. 9, September 1996

Interaction of Supersonic Wing-Tip Vortices with a Normal Shock

Iraj M. Kalkhoran,* Michael K. Smart,† and Alexander Betti‡
Polytechnic University, Brooklyn, New York 11201

An experimental study involving interaction of concentrated streamwise wing-tip vortices and normal shock fronts was carried out in a Mach 2.49 flow. The interaction scheme involved positioning a vortex-generator wing section upstream of a pitot-type normal shock inlet such that the wing-tip vortices interacted with the normal shock formed in front of the inlet. The vortex strength was varied by placing the vortex generator wing at different angles of attack while a normal shock was created by adjusting the mass flow rate passing through the inlet. Spark shadowgraphs, laser sheet planar visualizations, and pitot pressure measurements of the flowfield indicated a significant change in the structure of streamwise vortices generated by the vortex generator wing at 5.7- and 10.4-deg angle of attack upon encountering a normal shock discontinuity. Results of the investigation showed that the interactions lead to the formation of an unsteady conical shock wave far upstream of the inlet as well as a highly turbulent flow downstream for both vortices. Pitot pressure measurements using a fast response pressure transducer in conjunction with the spark shadowgraphs revealed a bimodal feature of the flowfield. The frequency of oscillation of the generated structure was found to be higher for increased vortex strength. Measurements of pitot pressure in the vortex core in the absence of a shock wave revealed high-frequency oscillations that were attributed to the vortex meandering phenomenon.

Introduction

THE interaction of a concentrated vortex and a shock wave may occur in many instances in the operational environment of supersonic aircraft and missiles. The interaction may be a result of vortices created by the forward components of a supersonic vehicle convecting downstream and interacting with shock waves formed over aft surfaces or shock waves present in front of the air intake system of the vehicle, leading to performance deterioration. In practice, such encounters involve interaction of three-dimensional curved line vortices with nonplanar shock fronts. Experimental evidence[1–6] indicates that the flowfield generated by the shock wave/vortex interaction can result in destruction of vortices with large-scale turbulent structure similar to those observed during low-speed vortex breakdown. Although the aerodynamic implications of the vortex breakdown in external and internal flows are in general undesirable, this phenomenon has been suggested as a potential means of enhancing the rate of fuel and air mixing in the combustor of a supersonic combustion ramjet (scramjet).

Previous experimental and numerical studies of the shock wave/vortex interaction problem have concentrated on a streamwise vortex interacting with an otherwise planar shock front with emphasis on supersonic vortex breakdown. Although interaction of a streamwise vortex with an oblique shock wave is more likely to occur in practice, prior studies have mainly dealt with interaction of a streamwise vortex with a normal shock wave in an attempt to establish a vortex breakdown limit as a function of vortex swirl rate and flow Mach number. This is because of the severity of the pressure jump imposed on the vortex by a normal shock wave in comparison to that of an oblique shock front. As a result, for a given vortex strength, breakdown of streamwise vortices is more likely to occur during a normal shock wave/vortex interaction than an oblique shock wave/vortex interaction. Moreover, the normal shock wave/vortex interaction may be considered as an axisymmetric flow, whereas the oblique shock wave/vortex interaction is fully three dimensional, leading to a more complex flow.

The original study in this area appears to have been done by Zatoloka et al.,[1] who experimentally studied the interaction between a streamwise vortex generated by a swept wing and a normal shock in front of a pitot-type inlet. The results of their exploratory investigation indicated that a conical shock forms as a result of the encounter downstream of which a vortex breakdown and a stagnation zone was reported. The experimental study of Ref. 1 considered only a single vortex, and no detailed measurements of the flowfield were reported. Moreover, the experimental arrangement was such that the vortex had weakened by crossing an oblique shock front before interacting with the main normal shock. The first comprehensive study of the normal shock wave/vortex interaction problem was performed by Delery et al.,[2] who placed a vortex generator wing in the subsonic portion of a supersonic nozzle, while a normal shock wave was created by a pitot-type inlet placed in the test section. The drawback of this approach to simulate the shock wave/vortex interaction problem was that the axial Mach number of the vortex increased during the expansion process in the nozzle, whereas its swirl Mach number remained nearly constant. Consequently, the generated vortices were weak in comparison to those found in practice. The results of their study produced a vortex breakdown limit as a function of vortex swirl rate and Mach number; however, no visualizations of the generated flowfield were presented in Ref. 2.

Other experimental studies involving the interaction of streamwise vortices with normal shocks were reported by Metwally et al.[3] and Cattafesta and Settles.[4] The vortices of Refs. 3 and 4 were generated by swirl vanes, and the strength of these vortices were varied by changing the vane angles. Their results indicated a highly unsteady flow regardless of the vortex strength. A weak interaction, characterized by perturbation of the main shock that bulged forward with a characteristic size on the order of the incoming vortex core diameter, and a strong interaction consisting of a much larger bulged forward shock structure were identified. The results of Refs. 3 and 4 further extended the vortex breakdown curve of Delery et al.[2] to cover a wider range of Mach numbers.

On the numerical side, a few contributions have dealt with the behavior of streamwise vortices upon encountering an abrupt pressure jump imposed by a normal shock wave. In Ref. 2, numerical solution of the normal shock wave/vortex interaction problem using the steady Euler equations was presented. These results indicated a good agreement with experimental observations in the absence of

Presented as Paper 95-2283 at the AIAA 26th Fluid Dynamics Conference, San Diego, CA, June 19–22, 1995; received July 22, 1995; revision received Nov. 7, 1995; accepted for publication Dec. 1, 1995.

*Associate Professor, Department of Mechanical, Aerospace, and Manufacturing Engineering. Member AIAA.

†Graduate Research Fellow, Department of Mechanical, Aerospace and Manufacturing Engineering; currently National Research Council Research Fellow, NASA Langley Research Center, Mail Stop 168, Hampton, VA 23681. Student Member AIAA.

‡Graduate Student, Department of Mechanical, Aerospace, and Manufacturing Engineering. Student Member AIAA.

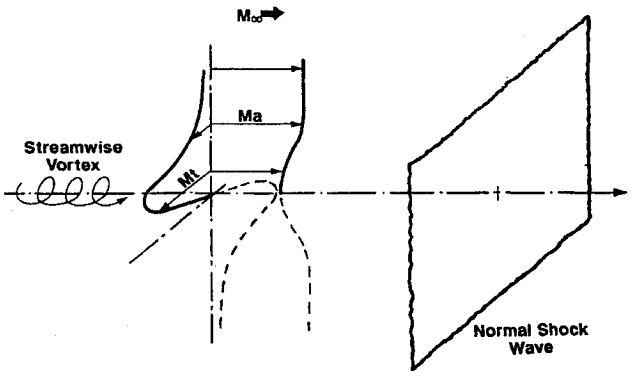

Fig. 1 Schematic representation of the normal shock wave/vortex interaction.

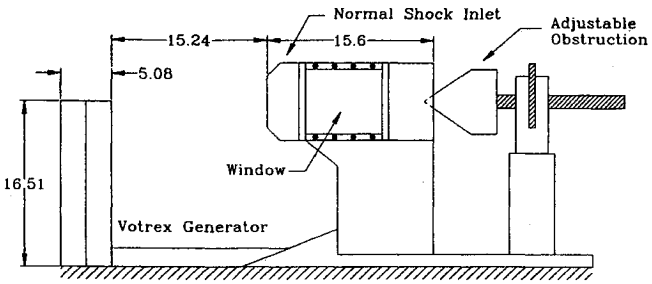

Fig. 2 Schematic of the experimental setup (side view); all dimensions are in centimeters.

vortex breakdown, and the breakdown limit was well predicted. Reference 3 reported the results of axisymmetric Navier–Stokes computations in support of the experimental data. These simulations predicted a similar structure to the strong interaction, including a stagnation point. Unsteady Navier–Stokes calculations were performed by Kandil et al.[7] for the case of quasiaxisymmetric vortices interacting with normal shocks in an inlet-type configuration that revealed several vortex breakdown modes.

Examination of the normal shock wave/vortex interaction problem (Fig. 1) reveals certain characteristics to be expected during such encounters. Since a planar normal shock wave is possible only for a flow with uniform properties upstream of the shock, any nonuniformity in the flow upstream of the shock wave will lead to a local deformation of the shock front. Consequently, introduction of a rotational vortex of limited spatial extent and nonuniform flow properties upstream of an otherwise planar normal shock will lead to local deformation of the shock, which in the absence of vortex breakdown will have a characteristic size on the order of the vortex core diameter. On the other hand, distortion of supersonic vortices have been experimentally shown to lead to formation of a subsonic conical structure with a characteristic size that is much larger than the vortex core diameter.[5]

The objective of the present work was to conduct an experimental study simulating the interaction of streamwise wing-tip vortices and normal shock waves in a Mach 2.49 flow. The experiments were designed to investigate behavior of vortices of various strengths encountering a severe pressure jump across a normal shock with particular emphasis on supersonic vortex distortion. A fundamental difference between the previous experimental studies of the normal shock wave/vortex interaction and that of the present investigation is the method used to generate the streamwise vortices. The vortices generated in the present study have been shown[8] to have different Mach number characteristics than those of previous work. In particular, the axial Mach number distribution in the core region of wing-tip vortices of the present work is considerably lower than that of the freestream, a fact that is believed to be of significance in the character of the resulting flowfield.

Test Facility, Instrumentation, and Experimental Setup

The experimental study of the interaction between streamwise vortices and normal shock waves was carried out in Polytechnic University's supersonic wind-tunnel facility.[9] The facility is an intermittent blowdown wind tunnel with a square test section of 38.1 × 38.1 cm and is capable of producing unit Reynolds numbers in the range of 26×10^6 to 22×10^7 per meter over a Mach number range from 1.75 to 4.0. The present experiments were performed at a nominal test section Mach number of 2.49. The stagnation pressure and temperature for these experiments were 0.45 MPa and 290 K, respectively, resulting in a unit Reynolds number of 4.3×10^7 per meter.

A generic illustration of the experimental arrangement is shown in Fig. 2. The vortex generator is a semispan wing having a diamond shape airfoil section with a chord length of 50.8 mm, a span of 165.1 mm, a half-angle of 8 deg, and angle of attack capability in the range of 0–10 deg. Vortices of different intensity could be generated by placing the wing section at various angles of attack. The present study utilized two different vortex strengths by placing the wing at 5.7- and 10.4-deg angles of attack. A normal shock, pitot-type inlet is placed approximately 152.4 mm, or three vortex-generator chords, downstream of the wing section. The normal shock generator has a square 63.5 × 63.5 mm inlet that is 156 mm long and is equipped with optical windows for flow visualization and measurement purposes (Fig. 2). A normal shock wave is created in front of the inlet by an adjustable downstream obstruction in the form of two-dimensional wedge section that chokes the flow coming out of the inlet.

A possible drawback of using this arrangement to generate streamwise vortices suitable to study shock wave/vortex interaction problems is that interference might occur due to the complex wave structure (shock or expansion waves) caused by the wing placed in a supersonic stream, thereby adversely influencing the flowfield ahead of the shock. However, the problem can be circumvented by placing the downstream shock wave generator such that strong disturbances (or their reflections from the tunnel walls) are behind the interaction region. This was addressed in a previous study where experimental multihole conical probe measurements in the vortex core[8] and numerical simulation of the same problem indicated that outside of the vortex core the flow is essentially that of the freestream and the wave interference for the present configuration is not significant.[10] Effectiveness of the geometry of the present experimental arrangement to simulate the interaction problem has also been demonstrated in previous studies of supersonic vortex interaction problems.[5,6]

Quantitative measurements in the interaction region of the flowfield were conducted by means of a pitot probe equipped with a fast response pressure transducer to gain insight into the unsteady behavior of the flowfield. The pitot tube had a circular opening of 1.4 mm that diverged to a larger opening a short distance downstream of the nose to house the miniature pressure transducer. The probe was placed approximately 108 mm downstream of the vortex-generator wing section. The pitot pressure measurements were made using a fast response Kulite pressure transducer (Model XCQ-062-50A) that was installed in the probe shaft. The pressure transducer had an outer diameter of 1.6 mm, a useful range of 0–345 kPa, and a natural frequency response of 60 kHz. The amplified output from the transducer was digitized using a LeCroy 12-bit A/D convertor at rates up to 30 kHz. Conventional uncertainty analysis of the measurements indicated an uncertainty value of 0.066 for the Mach number and 0.0042 for the nondimensional pitot pressure (p_t/p_0).

Shadowgraphs of the flow were taken using a spark light source that provided microsecond range exposure times. Multiple spark shadowgraphs of the flowfield were possible at a rate of two per second. The output from the spark source was also fed into the data acquisition system to correlate the exact timing of the shadowgraphs with the measured pitot pressure during a typical run. Planar visualization of the flowfield were made using a ruby pulsed laser with a pulse duration on the order of 30 ns. A thin (on the order of 2 mm) laser sheet illuminates the segment of interest in the test section to provide planar visualization of the flowfield. For these tests, the flow was seeded using a mixture of water and alcohol (two-thirds water and one-third alcohol by volume) in the settling chamber before the tunnel start. These planar visualizations were performed at several axial locations downstream of the vortex generating wing.

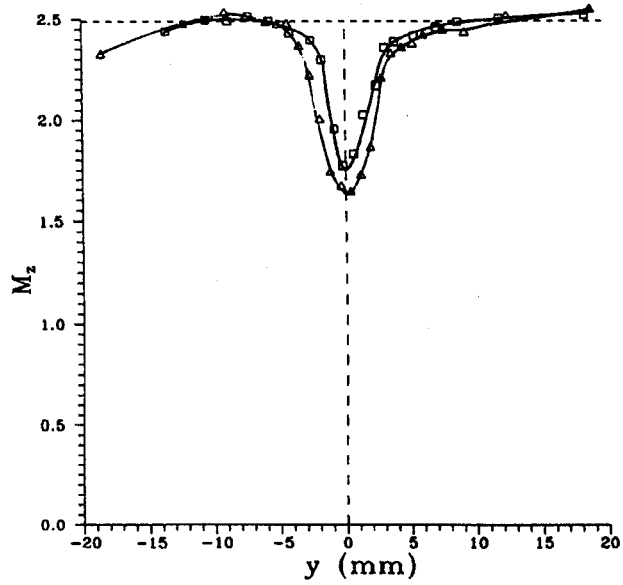

Fig. 3 Distribution of the axial Mach number in the vortex: □, α = 5 deg; △, α = 10 deg; and - - -, freestream.

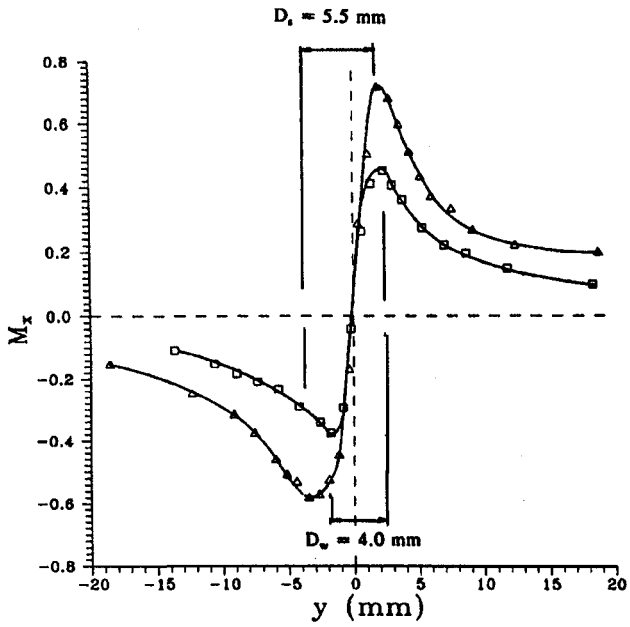

Fig. 4 Distribution of the tangential Mach number in the vortex: □, α = 5 deg and △, α = 10 deg.

Experimental Results

Characteristics of Wing-Tip Vortices

Measurements of flow properties in the core region of supersonic wing-tip vortices by means of conical five-hole and four-hole probes were conducted in a previous study.[8] These measurements were made for vortices generated by the wing placed at 5.7-deg (weak vortex) and 10.4-deg (strong vortex) angles of attack at a distance of 113 mm (2.25 chords) downstream of the vortex generator trailing edge. The results indicated a significant deficit in the axial Mach numbers and total pressures along with Burger-like swirl distributions for both vortices.[8] Figures 3 and 4 illustrate the axial and swirl components of the Mach number in the core region of vortices, respectively. These figures also indicate tightly wound vortices with viscous core diameters of approximately 4 mm for the weak vortex and 5.5 mm for the strong vortex. The axial Mach number distributions show a wakelike profile with a minimum axial Mach number of 1.75 and 1.63 for the weak and strong vortices, respectively. Such deficits are believed to play a strong role in the character of the shock wave/vortex interaction problem. As already stated, no evidence of shock/expansion waves from the vortex generating wing is present.

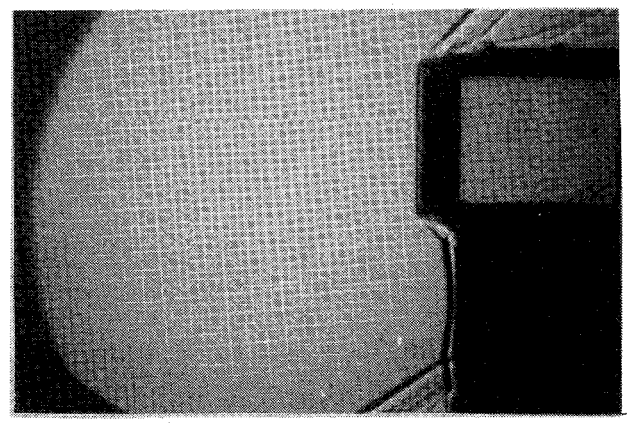

Fig. 5 Shadowgraph of the flow resulting in the formation of a planar normal shock.

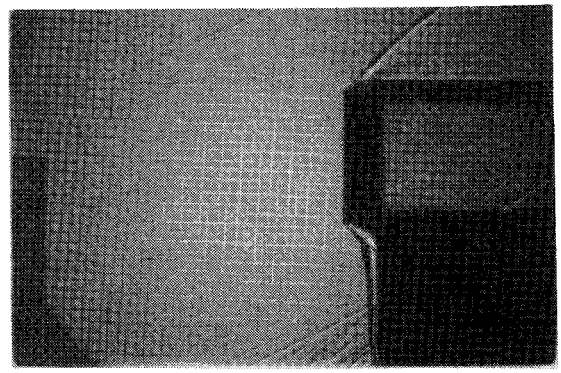

Fig. 6 Shadowgraph of the flow illustrating the vortex passing through the inlet.

Results for the Weak Vortex

The initial experiments were carried out to investigate feasibility of the experimental setup to effectively simulate the normal shock wave/vortex interaction problem. These experiments included visualization of the generated flowfield in the absence of the vortex to determine the proper blockage needed to create a planar normal shock wave. Figure 5 is a shadowgraph of the flowfield in which a planar normal shock is created by properly adjusting the downstream choke obstruction. The interaction experiments were initiated by placing the vortex generator wing section at an angle of attack of 5.7 deg upstream of the normal shock inlet. The strength of this vortex was the weaker of the two vortices considered during previous experiments dealing with the interaction of wing-tip vortices and oblique shock fronts.[6] In the experiments of Ref. 6, interaction of this vortex with the strongest attached planar oblique shock at Mach 2.49 did not reveal significant alterations to the structure of the vortex, and the vortex was seen to pass smoothly through the oblique shock.

Figure 6 is a shadowgraph of the flowfield taken when the vortex generator is placed upstream of the normal shock inlet. A concentrated wing-tip vortex may be seen in the shadowgraph that convects downstream and is seen to pass through the inlet. Figure 6 indicates that introduction of the vortex reduces the mass flow rate upstream of the inlet, which causes the inlet flow to unchoke and the shock wave to be swallowed. This is caused by the reduced axial velocity in the vortex core in comparison to the undisturbed flow. As a result, it was necessary to slightly increase the downstream blockage for the interaction experiments involving wing-tip vortices to ensure choked flow through the inlet. Experimental evidence indicated that an increase of the inlet blockage beyond the minimum value required to choke the flow had no effect on the character of the resulting flowfield during the shock wave/vortex interaction studies. Figure 7a shows a spark shadowgraph of the flowfield generated as a result of the interaction. In that picture, the vortex may be seen to expand drastically downstream of a conical shock structure. The forward

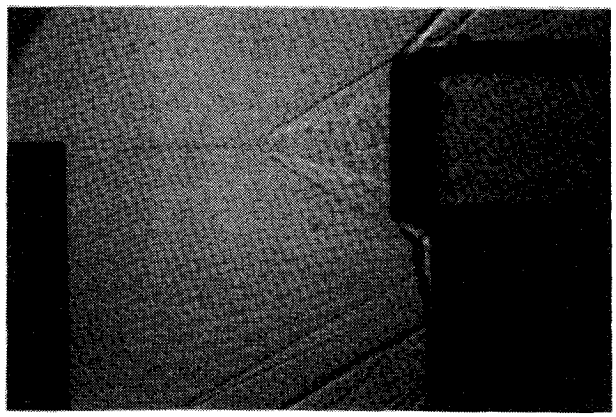

Fig. 7a Shadowgraph of the flow during a weak vortex/shock wave interaction at $t = t_1$.

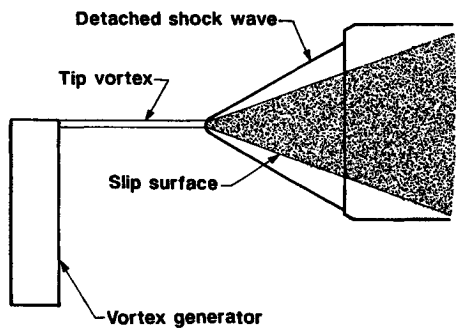

Fig. 7b Interpretation of the shadowgraph observed in Fig. 7a.

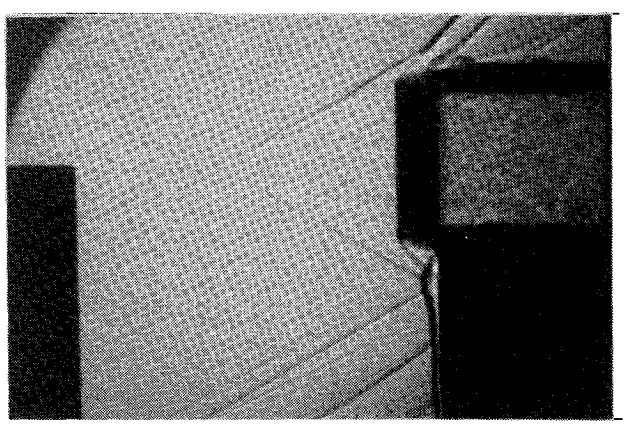

Fig. 7c Shadowgraph of the flow during a weak vortex/shock wave interaction at $t = t_2$.

portion of the conical shock wave is situated approximately 80 mm upstream of the inlet, suggesting the strong influence of the subsonic flow inside the inlet on the character of the resulting flowfield.

The generated flow may be seen to have a strong visual resemblance to the distorted vortex structure observed during the head-on interaction of a streamwise vortex and a wedge[5] and those observed during the strong oblique shock wave/vortex interactions reported in Ref. 6. One notable exception between the present results and those of Ref. 6 is the larger scale of the conical structure observed during the normal shock/vortex interaction in comparison to those observed during the oblique shock wave/vortex interactions. This difference is believed to be caused by the larger scale of the subsonic flow downstream of the normal shock that is capable of propagating information upstream as opposed to that observed during the oblique shock/vortex interaction tests. In the present configuration, the entire inlet (which has a scale much larger than that of the incoming vortex core diameter) is subsonic and is therefore capable of influencing the upstream flow, whereas the oblique shock/vortex interaction experiments of Ref. 6 revealed a structure containing subsonic flow of much smaller size that may influence the upstream flow. In Ref. 5, the flow leading to vortex distortion was suggested to consist of two distinct regions: a central subsonic zone consisting of the distorted vortex with its apex situated at the vortex center and a supersonic region formed between the distorted vortex and the conical shock structure. Similar to the observations of Ref. 5, the subsonic conical region formed as a result of vortex distortion may be interpreted as a solid conical body placed in a supersonic stream resulting in the formation of a detached conical shock wave in a manner similar to the supersonic flow over a conical surface. An interpretation of the flowfield generated during the normal shock wave/vortex interaction based on the vortex distortion model of Ref. 5 is presented in Fig. 7b. Note, however, that a fundamental difference between the present interaction and those of Ref. 5 is that a stagnation point is present on the wedge leading edge during the vortex wedge interaction experiments whereas the current configuration does not have a forced stagnation point. Examination of the shadowgraph shown in Fig. 7a and its comparison to that shown in Fig. 6 also indicates that the flow inside the inlet is highly turbulent and remains subsonic.

Multiple spark shadowgraphs of the flow during the normal shock wave/vortex interaction experiments indicated an unsteady behavior of the flowfield leading to formation of conical shock structures of different size. An example of this unsteady flow behavior may be observed by comparing the shadowgraph of Fig. 7a with that shown in Fig. 7c, which was taken during the same run but at a later time. However, the subsonic central region containing the distorted vortex was limited to the inlet area in all of the experiments performed during this study. This observation suggests that interaction of wing-tip vortices with normal shock fronts leading to vortex distortion is strongly governed by the extent of the subsonic region downstream of the undisturbed normal shock wave. Another important facet of the interaction leading to vortex distortion may be seen by examining Figs. 7a and 7c, which indicate a strongly curved shock in the vicinity of the vortex center whereas outside this region the shock may be seen to be straight. The length scale associated with the curved portion of the conical shock wave is seen to be on the order of the vortex viscous core diameter (about 4 mm for this case), suggesting that distortion of supersonic wing-tip vortices is largely a viscous phenomenon. In Ref. 5 the initial stage of vortex distortion during a head-on collision with a wedge was argued to be a result of Mach number and flow angularity distribution in the core of wing-tip vortices (i.e., inviscid in character). This resulted in a local detachment of the shock because of the inability of the wedge to support an attached shock wave leading to the formation of a subsonic region of limited spatial extent. The strong pressure jump across the detached shock wave was suggested to be responsible for distortion of vortices, whereas the subsonic region downstream of the shock allowed upstream transmission of disturbances, causing the shock to be situated far upstream of the wedge leading edge. The flowfield in the present investigation is also of similar character, and the observed vortex distortion is believed to be initiated predominantly by inviscid means (i.e., because of nonuniformity of flow properties upstream of the shock). However, once vortex distortion has occurred, the observed significant reorganization of the flowfield is expected to be dominated by viscous effects. This observation is of significant importance when considering inviscid computations of the interaction of wing-tip vortices with normal shock fronts as well as supersonic vortex dominated flows with vortex breakdown.

The shadowgraphs of Figs. 7a and 7c also indicate a significantly higher turbulence levels downstream of the conical shock structure as a result of shock wave/vortex interaction. Although a universally accepted feature of low-speed vortex breakdown is the formation of a highly turbulent region, a fundamental difference between incompressible vortex breakdown and vortex bursting in crossing a shock wave exists. An examination of the quasisteady state of the flowfield, similar to those seen in Figs. 7a and 7c, indicates that the normal shock wave/vortex interaction problem degenerates into the problem of a streamwise vortex crossing a highly curved shock structure with the shock being normal to the axial flow direction at the vortex axis. As a result, the degree of fluctuating turbulent components and Reynolds stresses in the vortex will be subject to amplification in crossing the strong shock wave in a manner similar to those observed during shock wave boundary-layer interactions,[11–13] as the vortical

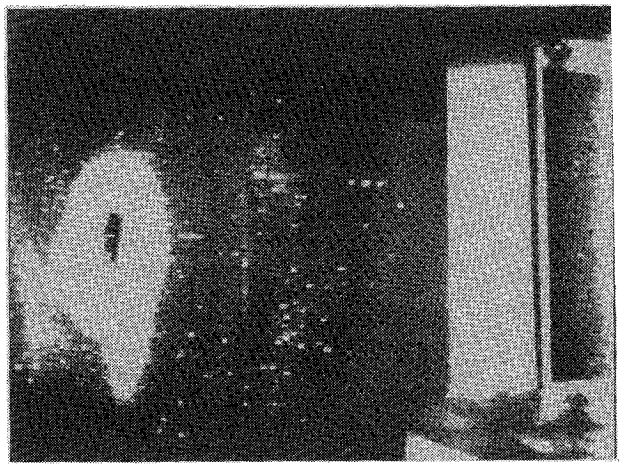

Fig. 8a Laser sheet visualization of the vortex slightly downstream of the conical shock.

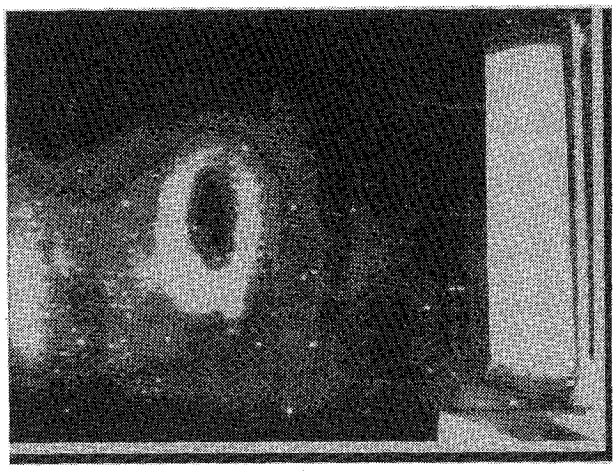

Fig. 8b Laser sheet visualization of the vortex far downstream of the conical shock.

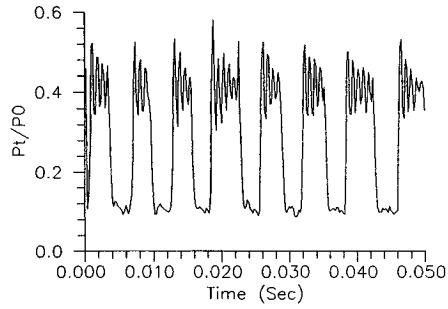

Fig. 9 Time history plot of the pitot pressure during the interaction of the weak vortex.

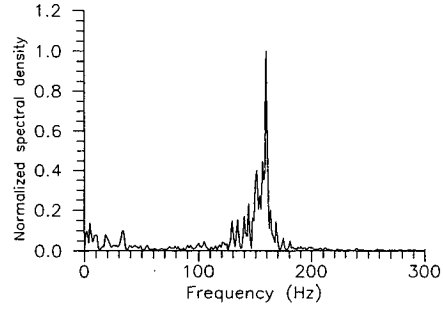

Fig. 10 Power spectral density distribution for the weak vortex/shock interaction.

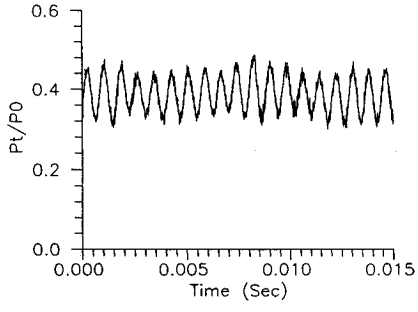

Fig. 11 Time history plot of the pitot pressure in the core of the weak vortex.

structure results from separation of the boundary layer. This is particularly important when applying a low-speed turbulence model in computational solutions of the shock wave/vortex interaction with vortex breakdown.

Planar laser-sheet visualizations of the flowfield during a typical interaction are illustrated in Figs. 8a and 8b at two different axial locations. Figure 8a is a slice of the flow slightly downstream of the conical shock structure. Figure 8b, on the other hand, represents planar visualization of the flow at an axial location far downstream of the conical shock. The aforementioned figures illustrate a significant growth of the vortex size with the downstream distance, which is also a known characteristic of the incompressible vortex breakdown. Furthermore, the lack of seed particles in the structure as evident by the dark regions demonstrates little mixing of the supersonic outer flow with the subsonic central region, which is in agreement with the flow model presented in Fig. 7b.

Further insight into the problem, particularly the unsteady character of the interaction, may be gained by considering the results of pitot pressure measurements. It should be mentioned that these measurements are not capable of providing details of the turbulent properties in the flow. Figure 9 illustrates the time history of the measured pitot pressure for a 50-ms period. In Fig. 9 and subsequent time history plots, $t = 0$ is arbitrary and represents the start of the data acquisition process, which is well after establishment of supersonic flow in the test section. The preceding figure representing measurements in a fixed point in space clearly demonstrates a bimodal character of the flow. One mode corresponds to the case for which the probe is upstream of the burst region (representing pitot pressure measurements of the undisturbed vortex), whereas the second mode represents the case for which the probe is inside the conical structure (i.e., distorted vortex). A similar observation was made in the experiments of Delery et al.[14] in a low-speed flow by means of laser Doppler velocimetry (LDV) measurements. In Ref. 14 a streamwise oscillation of the vortex breakdown point was observed that indicated the existence of two states at a fixed point in space. Examination of the standard power spectral density of the pitot pressure measurements at several sampling frequencies indicated a highly repeatable frequency of about 160 Hz associated with the occurrence of the two modes. An example of the normalized power spectral density distribution indicating the frequency distribution of the unsteady motion is shown in Fig. 10.

To associate the observed modes with the state of the flowfield, simultaneous measurements of the pitot pressure and spark shadowgraphs of the flow were obtained. Analysis of this procedure indicated that the first mode, representing the case for which the probe is upstream of the burst conical region, is characterized by a higher mean pitot pressure and relatively high-amplitude fluctuating pressures. On the other hand, the second mode, representing the case in which the probe is inside the conical structure, had a substantially lower mean value and lower amplitude pitot pressure fluctuations. At least two pieces of evidence exist to support this argument. First, the mode in which the probe is outside the conical region should closely correspond to that of the undisturbed vortex, which is argued to be the mode with higher mean pressure shown in Fig. 9. Measurements were performed in the undisturbed vortex core by removing the downstream inlet blockage and preventing the formation of a normal shock. An example of pitot pressure time history for this case covering a period of 15 ms is shown in Fig. 11. Comparison of pressure traces for mode 1, shown in Fig. 9, and measurements in the

Fig. 12a Shadowgraph of the flow and time history of the measured pitot pressure at $t = t_1$.

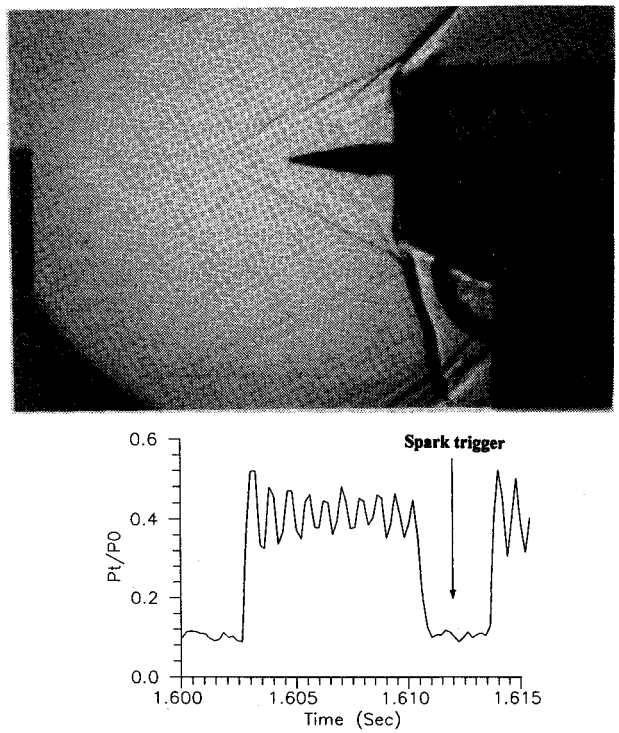

Fig. 12b Shadowgraph of the flow and time history of the measured pitot pressure at $t = t_2$.

vortex core, illustrated in Fig. 11, demonstrates close agreements in terms of amplitude, frequency, and mean values. The second and stronger evidence supporting the aforementioned argument is obtained by correlating the exact time at which the shadowgraphs were taken with the measured pitot pressure. This is illustrated in Figs. 12a and 12b at two distinct time intervals during the same run. The instant at which the spark light source for the shadowgraphs is activated and the shadowgraphs corresponding to them are also shown in Figs. 12a and 12b.

Figure 11 also indicates a relatively high-frequency (approximately 1.2 kHz) and amplitude fluctuations about a mean value of $p_t/p_0 = 0.39$ in comparison to that of the empty test section that has a value of 0.50. The lower value of pitot pressure relative to that of the freestream is in agreement with the conical probe measurements of Ref. 8 in the core of the vortex. However, the fluctuations of pitot pressures were not detected in the measurements of Ref. 8 because of the damping effect of conventional probes with finite tubing length. These fluctuations are believed to be caused by the vortex meandering phenomenon, and since gradients of flow properties in the vortex core are large,[8] any slight meander of the vortex will produce large-amplitude pitot pressure fluctuations. A similar type of vortex meander was observed during the head-on interaction of a wing-tip vortex with a wedge in a Mach 3 flow.[5] In contrast to mode 1, the second mode in which the probe is immersed in the conical burst region has significantly lower mean ($p_t/p_0 \approx 0.1$) and fluctuating pressures. Although the exact cause of this observation is not well understood at the present time, a candidate mechanism to explain this behavior may be the formation of a reversed flow and a stagnation region in the burst structure, which is a universally accepted characteristic of incompressible vortex breakdown. More detailed measurements of this region using other techniques are needed to substantiate this argument.

Results for the Strong Vortex

Interaction experiments incorporating stronger wing-tip vortices were carried out by placing the vortex generator at an angle of attack of 10.4 deg. The axial and swirl Mach number distributions for the 10.4-deg vortex as reported in Ref. 8 were shown in Figs. 4 and 5, respectively. In contrast to the weak vortex experiments, interaction of this vortex with a strong oblique shock in a Mach 2.49 flow revealed a significant expansion of the vortex core downstream of a separated shock structure.[6] Successive spark shadowgraphs of the flowfield during a typical run for this strong encounter are presented

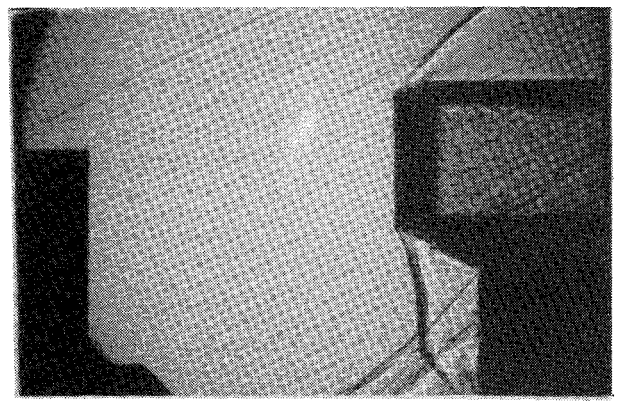

Fig. 13a Shadowgraph of the flow during a strong vortex/shock wave interaction at $t = t_1$.

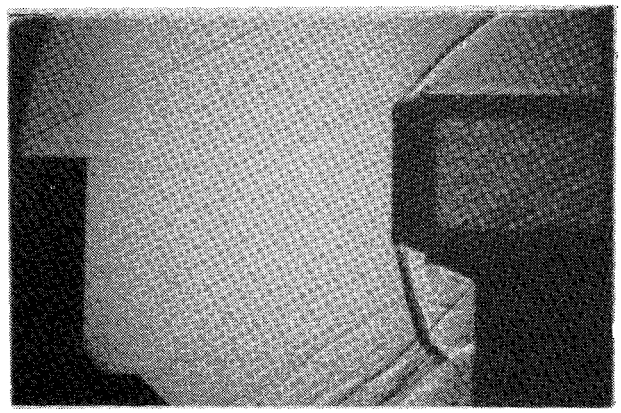

Fig. 13b Shadowgraph of the flow during a strong vortex/shock wave interaction at $t = t_2$.

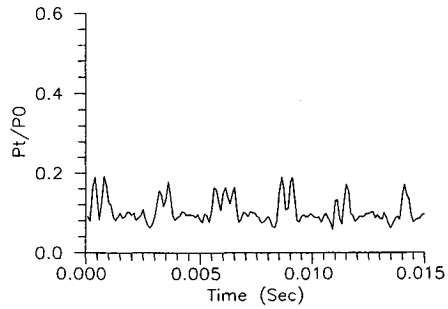

Fig. 14 Time history plot of the pitot pressure during the interaction of the strong vortex.

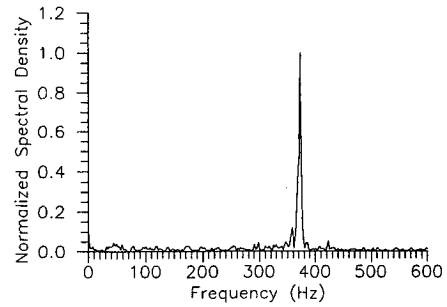

Fig. 15 Power spectral density distribution for the strong vortex/shock interaction.

in Figs. 13a and 13b. The flow may be seen to have a strong visual resemblance to the 5.7-deg case discussed earlier. The length scale associated with the curved portion of the conical shock wave is again seen to be on the order of the vortex viscous core diameter. Similar to the 5.7-deg case, the unsteady nature of the flow together with the formation of a conical and highly turbulent region are also apparent.

A notable difference between the strong and weak vortex interactions does, however, exist. Figure 14 is a time history plot of the measured pitot pressure for a period of 15 ms. An examination of that figure indicates a higher frequency associated with the two modes and a substantially lower mean pitot pressure in mode 1 relative to the 5.7-deg case. The lower mean pitot pressure measured is again consistent with the measurements of Ref. 8 for the stronger vortex. The frequency of occurrence for the two modes as indicated by the normalized power spectral density distribution shown in Fig. 15 has more than doubled for this case (on the order of 375 Hz), whereas the distinction between the modes is not as clear as the 5.7-deg case. Conversely, the mean value of the measured pitot pressures for mode 2 is approximately the same as the one observed for the weak vortex (0.09 for the strong vortex vs 0.1 for the weak vortex). In summary, interaction experiments involving the strong vortex exhibited many characteristics of the weak vortex case that was discussed earlier.

Study of the pitot pressure history plots for the interaction of weak (Fig. 9) and strong (Fig. 14) vortices reveals yet another feature of the conical structure. The aforementioned figures indicate an almost instantaneous transition from one mode to the next, as is evident from a sharp increase or decrease of the measured pitot pressures. This trend and the shadowgraphs shown in Fig. 12 suggest that the pitot pressure remains nearly constant with the downstream distance starting immediately behind the conical shock for interactions involving both vortices.

Conclusions

An exploratory experimental study involving interaction of concentrated streamwise wing-tip vortices and normal shock fronts was carried out in a Mach 2.49 flow. Spark shadowgraphs, laser sheet planar flow visualizations, and pitot pressure measurements incorporating a fast response pressure transducer indicate a significant change in the structure of streamwise vortices upon encountering a normal shock wave. These observations reveal that the interaction leads to the formation of an unsteady conical shock wave far upstream of the inlet as well as a highly turbulent flow downstream. Time accurate measurements of the pitot pressure in conjunction with the spark shadowgraphs reveal a bimodal feature of the flowfield. Although many features of the interaction experiments incorporating weak and strong vortices are identical, some differences in details of the unsteady flow are observed. Interaction of a strong wing-tip vortex with a normal shock indicated higher frequency oscillations than those of the weak vortex. Measurements of pitot pressure in the vortex core in the absence of a shock wave reveal high-frequency oscillations caused by the vortex meandering phenomenon.

Acknowledgments

This work was supported by the U.S. Air Force Office of Scientific Research under Grant F49620-94-1-0210 and NASA Lewis Research Center under Grant NAG3-1378. The assistance provided by Lester Orlick and Svetozar Popovic was greatly appreciated during the experimental study.

References

[1]Zatoloka, V., Ivanyushkin, A. K., and Nikolayev, A. V., "Interference of Vortexes with Shocks in Airscoops. Dissipation of Vortexes," *Fluid Mechanics—Soviet Research*, Vol. 7, No. 4, 1978, pp. 153–158.

[2]Delery, J., Horowitz, E., Leuchter, O., and Solignac, J. L., "Fundamental Studies on Vortex Flows," *La Recherche Aerospatiale* (English Edition), No. 2, 1984, pp. 1–24 (ISSN 0379-380X).

[3]Metwally, O., Settles, G., and Horstman, C., "An Experimental Study Wave/Vortex Interaction," AIAA Paper 89-0082, Jan. 1989.

[4]Cattafesta, L. N., and Settles, G. S., "Experiments on Shock/Vortex Interaction," AIAA Paper 92-0315, Jan. 1992.

[5]Kalkhoran, I. M., "Vortex Distortion During Vortex-Surface Interaction in a Mach 3 Stream," *AIAA Journal*, Vol. 32, No. 1, 1994, pp. 123–129.

[6]Smart, M. K., and Kalkhoran, I. M., "Effect of Shock Strength on Oblique Shock-Wave/Vortex Interaction," *AIAA Journal*, Vol. 33, No. 11, 1995, pp. 2137–2143; also AIAA Paper 95-0098, Jan. 1995.

[7]Kandil, O. A., Kandil, H. A., and Liu, C. H., "Supersonic Quasi-Axisymmetric Vortex Breakdown," AIAA Paper 91-3311, Sept. 1991.

[8]Smart, M. K., Kalkhoran, I. M., and Bentson, J., "Measurements of Supersonic Wing Tip Vortices," *AIAA Journal*, Vol. 33, No. 10, 1995, pp. 1761–1768; also AIAA Paper 94-2576, June 1994.

[9]Kalkhoran, I. M., Cresci, R. J., and Sforza, P. M., "Development of Polytechnic University's Supersonic Wind Tunnel Facility," AIAA Paper 93-0798, Jan. 1993.

[10]Rizzetta, D. P., "Numerical Investigation of Supersonic Wing-Tip Vortices," AIAA Paper 95-2282, June 1995.

[11]Anyiwo, J. C., and Bushnell, D. M., "Turbulence Amplification in Shock-Wave Boundary-Layer Interaction," *AIAA Journal*, Vol. 20, No. 7, 1982, pp. 893–899.

[12]Zang, T. A., Hussaini, M. Y., and Bushnell, D. M., "Numerical Computations of Turbulence Amplification in Shock-Wave Interactions," *AIAA Journal*, Vol. 22, No. 1, 1984, pp. 13–21.

[13]Trolier, J. W., and Duffy, R. E., "Turbulence Measurements in Shock-Induced Flows," *AIAA Journal*, Vol. 23, No. 8, 1985, pp. 1172–1178.

[14]Delery, J., Pagan, D., and Solgnac, J. L., "On the Breakdown of the Vortex Induced by a Delta-Wing," *Vortex Control and Breakdown Behavior*, Second International Colloquium on Vortical Flows, Baden, Switzerland, 1987.